Muonic Molecules in Liquid Hydrogen*

E. J. BLESER,† E. W. ANDERSON, L. M. LEDERMAN, S. L. MEYER,
J. L. ROSEN, J. E. ROTHBERG,‡ AND I-T. WANG
Columbia University, New York, New York

(Received 31 July 1963)

We have studied the yield and time distribution of 5.5-MeV gamma rays from the fusion reaction $p+d \rightarrow He^3+\gamma$. The reaction was catalyzed by muons from the Nevis synchrocyclotron which were stopped in a target containing high-purity liquid hydrogen. A digitron of 30-nsec resolving time was used to study the yield of gamma rays as a function of the time that elapsed between the stopping of a muon and the emission of a gamma ray and as a function of the deuterium concentration, which was varied from 1 ppm to 25%. Analysis of the experimental distributions gives rates (in sec^{-1}) for the following muonic molecular processes:

$$\begin{aligned} p\mu+p &\rightarrow p\mu p, & \lambda_{pp} &= (1.89\pm0.20)\times10^6,\\ p\mu+d &\rightarrow d\mu+p, & \lambda_e &= (1.43\pm0.13)\times10^{10},\\ d\mu+p &\rightarrow p\mu d, & \lambda_{pd} &= (5.80\pm0.30)\times10^6,\\ p\mu d &\rightarrow He^3+\gamma, & \lambda_f &= (0.305\pm0.010)\times10^6. \end{aligned}$$

The yield of fusion gamma rays was observed to increase with increasing deuterium concentration until it reached a saturation value of $(14.0\pm2.4)\%$ at 1% concentration. At 25% deuterium concentration the yield was observed to increase by a factor of 1.17 ± 0.01 above the saturation yield. This effect is in agreement with a prediction of Wolfenstein and Gershtein. When neon was in solution in the hydrogen at a concentration of 1%, all of the muons transferred to the neon and the disappearance rate of muons bound to neon was measured to be $(0.658\pm0.010)\times10^6$ sec^{-1}.

I. INTRODUCTION

SINCE the muon is similar to an electron in all respects, except for its mass, atoms and molecules can be formed which have one of their electrons replaced by a negative muon. These muonic atoms and molecules are analogous to the corresponding electronic systems, but since the mass of the muon is 207 electron masses, its Bohr orbit radius is 207 times smaller than the Bohr orbit radius of the electron. The close binding of the muon results in some properties of the muonic systems quite different from those of electronic systems. This paper reports an experiment which studied the atomic and molecular processes of negative muons in liquid hydrogen.

To investigate these processes, we use an event in which a proton and a deuteron, bound in a molecule by a muon, are bound so closely that they may fuse, forming He^3 with the emission of a 5.5-MeV gamma ray. It is possible for as many as 15% of the muons that stop in a liquid-hydrogen target to catalyze fusion reactions. The resulting gamma rays can be studied, not only as a function of deuterium concentration, but also as a function of the time that elapses between the stopping of a muon in the hydrogen and the production of a gamma ray. The purpose of this experiment was to measure the formation rates of the μd and μNe muonic atoms and the $p\mu p$ and $p\mu d$ muonic molecules, and to measure the fusion rate of a proton and a deuteron bound in an S state by a muon.

These rates have intrinsic interest, many theoretical attempts having been made to calculate them.[1] In addition, knowledge of these rates is necessary to understand the results of the important experiments which seek to determine the form of one of the basic weak interactions

$$\mu^-+p \rightarrow n+\nu$$

by studying muon capture in hydrogen. The present experiment was carried out in conjunction with an experiment which studied muon capture in hydrogen.[2]

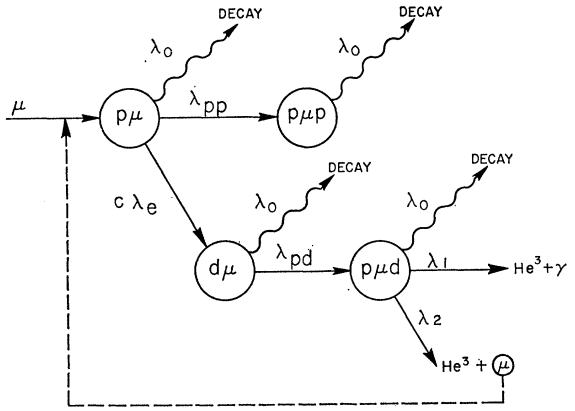

FIG. 1. Schematic diagram of the steps leading to a fusion event and of the important alternate processes for the case c (the deuterium concentration) $\ll1$ and negligible impurity concentration. The decay rate is $\lambda_0=0.455\times10^6$ sec^{-1}. The conversion muon set free by a fusion event can start the process over again.

* Work supported in part by the Office of Naval Research.

† Present address: Brookhaven National Laboratory, Upton, New York.

‡ Present address: Yale University, New Haven, Connecticut.

[1] Ya. B. Zeldovich and S. S. Gershtein, Usp. Fis. Nauk **71**, 581 (1960) [English transl.: Soviet Phys.—Usp. **3**, 593 (1961)]. This paper is a review article of all the work in the field prior to 1960.

[2] The preceding paper, J. E. Rothberg, E. W. Anderson, E. J. Bleser, L. M. Lederman, S. L. Meyer, J. L. Rosen, and I. T. Wang, Phys. Rev. **132**, 2664 (1963). Also, E. Bleser, L. Lederman, J. Rosen, J. Rothberg, and E. Zavattini, Phys. Rev. Letters **8**, 288 (1962).

II. BACKGROUND

A. Muonic Processes in Liquid Hydrogen

A muon stops in liquid hydrogen forms a muonic hydrogen atom and cascades to the ground state of the atom in less than 10^{-9} sec.[3] The muonic hydrogen atom (μp) is a neutral object of small dimensions and its motion through matter is therefore like that of a neutron in that it penetrates through the electron shells of an atom to interact with the nucleus. There is a high probability that the muon will transfer from the proton to the other nucleus.[4] If the second nucleus is a deuteron or an impurity in the hydrogen with Z greater than 1, the transfer process is irreversible, since the available thermal energy (0.002 eV) is much less than the increase in the binding energy. The reduced mass effect increases the binding energy of the μd system by 135 eV over that of the μp system.

In addition to the muon transfer processes, the μp system can form a muonic molecule with another proton. The normal decay of a muon into an electron and two neutrinos and the weak interaction capture of the muon by the proton are also possible. Since the decay rate is 10^3 times the capture rate in hydrogen, we ignore the capture process in this paper. Thus the channels by which the μp system can change are:

(1) The muon can decay to an electron and two neutrinos with a rate equal to the decay rate of the positive muon ($\lambda_0=0.455\times10^6$ sec^{-1}).

(2) The muon can transfer to an impurity (Z) with a rate $c_z\lambda_z$ [c_z is the concentration of impurity, λ_z is the transfer rate for a muon from a proton to an impurity atom (Z) when $c_z=1$].

(3) The muon can transfer to a deuteron with a rate $c\lambda_e$ (c is the concentration of deuterium, λ_e is the transfer rate for a muon from a proton to a deuteron in liquid deuterium).

(4) The μp system can combine with another proton to form a $p\mu p$ molecule (ion) at a rate $(1-c)\lambda_{pp}$, where λ_{pp} is the rate of molecular formation in pure liquid hydrogen.

(5) The μp system can combine with a deuteron to form a $p\mu d$ molecule (ion), but this process can be ignored since the probability that the muon will transfer from the proton to the deuteron is 10^4 times greater. Figure 1 shows these and the succeeding processes, the unimportant channels being suppressed.

If the muon is bound to an impurity ($Z>1$) or in a $p\mu p$ molecule, it can undergo no further molecular transitions since the system is charged and cannot penetrate neighboring atoms. From these states the muon must either decay or take part in the weak interaction. However, for the μd atom there are a number of channels:

(a) The muon can decay.

(b) The μd system can combine with a proton to form a $p\mu d$ molecule (ion) at a rate $(1-c)\lambda_{pd}$.

(c) The μd can combine with a deuteron to form a $d\mu d$ molecule (ion) at a rate $c\lambda_{dd}$.

(d) The muon can transfer to an impurity of higher Z at a rate $c_z\lambda_{dz}$. The transfer rate to impurities is not the same for μd and μp.[5]

The formation of the $d\mu d$ molecule can be ignored since λ_{dd} is small and $c\ll1$. The formation of μd, proportional to $c\lambda_e$, is important since λ_e is 10^4 times greater than the molecular formation rates. For high deuterium concentrations the $d\mu d$ molecule is still unimportant since it immediately fuses giving

$$d\mu d \rightarrow p+\mathrm{H}^3+\mu$$
$$\rightarrow n+\mathrm{He}^3+\mu.$$

Our gamma ray detecting system does not respond to this fusion process and the time distribution of the gamma rays is unchanged since the muon spends negligible time in the $d\mu d$ molecule.

The $p\mu d$ system can undergo no further molecular transitions because of its charge, but since the proton and the deuteron are bound very closely by the muon it becomes possible for them to tunnel through the Coulomb barrier and fuse to form He^3. The reaction is

$$p\mu d \xrightarrow{\lambda_1} \mu\,\mathrm{He}^3+\gamma, \tag{1a}$$

$$\xrightarrow{\lambda_2} \mathrm{He}^3+\mu. \tag{1b}$$

The fusion process releases 5.5 MeV of energy which is carried off by a gamma ray or by the conversion muon. This process was discovered in 1957 in a bubble chamber at Berkeley[6] when it was observed that stopping muons were rejuvenated with 5 MeV energy. The discovery stimulated several experiments and calculations, which are reviewed in Ref. 1. Tables I and II give some of the theoretical results and Table III gives experimental results, including those from a number of experiments more recent than Ref. 1.

B. Formulas

Figure 1 diagrams the steps leading to a fusion event, including the important alternate channels but

[3] A. Wightman, Phys. Rev. **77**, 521 (1950); J. H. Doede, R. H. Hildebrand, M. H. Israel, and M. R. Pyka, *ibid.* **129**, 2808 (1963).

[4] If the other nucleus is a proton an observable effect takes place since the muonic hydrogen atom is initially formed in two hyperfine states $J=1$ and $J=0$. The transfer process results in the muon being trapped in the lower energy $J=0$ state. The triplet state is depopulated in 10^{-10} sec [S. S. Gershtein, Zh. Eksperim. i Teor. Fiz. **34**, 463 (1958) (English transl.: Soviet Phys. —JETP **7**, 318 (1958))]. This depolarization of muons in liquid hydrogen has been observed by A. Ignatenko, L. B. Egorov, B. Khalupa, and D. Chultem, Zh. Eksperim. i Teor. Fiz. **35**, 894 (1958) [English transl.: Soviet Phys.—JETP **8**, 621 (1959)].

[5] M. Schiff, Nuovo Cimento **22**, 66 (1961).

[6] L. W. Alvarez, H. Bradner, F. S. Crawford, Jr., J. A. Crawford, P. Falk-Variant, M. L. Good, J. D. Gow, A. H. Rosenfeld, F. Solmitz, M. L. Stevenson, H. K. Ticho, and R. D. Tripp, Phys. Rev. **105**, 1127 (1957).

TABLE I. Some calculated values for the various molecular rates.[a]

	Refs. b	c	d	e
λ_e (10^{10} sec^{-1})	1.37	1.44	1.4	1.43
λ_{pp} (10^6 sec^{-1})	7.8	1.61	3.9	2.6
λ_{pd} (10^6 sec^{-1})	3.0	0.71	3.0	1.3
λ_{dd} (10^6 sec^{-1})	0.071	0.006	0.036	0.01

[a] Reported for density of hydrogen atoms of 4.2×10^{22} cm^{-3}.
[b] See Ref. 7.
[c] V. B. Belyaev, S. S. Gershtein, B. N. Zakharev, and S. P. Lomnev, Zh. Eksperim. i Teor. Fiz. **37**, 1652 (1959) [English transl.: Soviet Phys.—JETP **10**, 1171 (1960)].
[d] See Ref. 1 (derived from b).
[e] See Ref. 1 (derived from c).

TABLE II. Some calculated values for the fusion rate.

	Refs. c		d	e	f
R[a] (10^{-13} cm)	0	5	12		
λ_f[b] (10^6 sec^{-1})	0.18	0.26	0.48	0.26	0.6	10

[a] R = the sum of the nuclear radii.
[b] In the present paper λ_f is the fusion rate for the pd spin $\frac{1}{2}$ state while in Refs. c and d it is the fusion rate averaged over all spin states.
[c] J. D. Jackson, Phys. Rev. **106**, 330 (1957).
[d] S. Gallone, G. M. Prosperi, and A. Scotti, Nuovo Cimento **6**, 168 (1957).
[e] C. Hayashi, T. Nakano, M. Nishida, S. Suekano, and Y. Yamaguchi, Progr. Theoret. Phys. (Kyoto) **17**, 615 (1957).
[f] See Ref. 7.

assumes c_z is zero. Neglecting the effects of the recycling of the conversion muon and the hyperfine structure of the $p\mu d$ molecule, the yields of fusion gamma rays and conversion muons are:

$$n_\gamma=\left(\frac{c\lambda_e}{c\lambda_e+\lambda_{pp}+\lambda_0}\right)\left(\frac{\lambda_{pd}}{\lambda_{pd}+\lambda_0}\right)\left(\frac{\lambda_1}{\lambda_1+\lambda_2+\lambda_0}\right); \quad (2)$$

$$n_\mu=\left(\frac{c\lambda_e}{c\lambda_e+\lambda_{pp}+\lambda_0}\right)\left(\frac{\lambda_{pd}}{\lambda_{pd}+\lambda_0}\right)\left(\frac{\lambda_2}{\lambda_1+\lambda_2+\lambda_0}\right). \quad (3)$$

The Berkeley group[6] measured n_μ, the fraction of incident muons that are rejuvenated, as a function of c, and found that it increased with c until it reached a maximum value at 2% deuterium concentration. Thus at $c=0.02$, $c\lambda_e\gg\lambda_{pp}+\lambda_0$ and the fraction of incident muons that transfer to deuterons is close to 1. The solution of the set of coupled differential equations derived from Fig. 1 (Appendix I) gives the yield of gamma rays as a function of the time that elapses between the stopping of the muon and the emission of a gamma ray.

$$(d/dt)n_\gamma(t)=\lambda_1\lambda_{pd}c\lambda_e e^{-\lambda_0 t}\left\{\frac{e^{-\alpha t}}{(\alpha-\lambda_{pd})(\alpha-\lambda_f)}+\frac{e^{-\lambda_{pd}t}}{(\alpha-\lambda_{pd})(\lambda_f-\lambda_{pd})}-\frac{e^{-\lambda_f t}}{(\alpha-\lambda_f)(\lambda_f-\lambda_{pd})}\right\}, \quad (4)$$

TABLE III. Experimental values of molecular and fusion rates.

	Refs. a	b	c	d	e	f	g	This experiment
λ_e (10^{10} sec^{-1})					1.9 ±0.7	$1.2_{-0.2}{}^{+0.4}$		1.43 ±0.13
λ_{pp} (10^6 sec^{-1})					1.4 ±0.5		2.81±0.16 and 3.26±0.78	1.89 ±0.20
λ_{pd} (10^6 sec^{-1})		$0.55<\lambda<20$	>10		5.5 ±1.1	$0.5_{-0.4}{}^{+0.6}$	6.55±0.46 7.18±0.67 7.75±0.77	5.8 ±0.3
λ_{dd} (10^6 sec^{-1})						0.44±0.14		
λ_f (10^6 sec^{-1})		$0.19<\lambda<0.88$			0.26±0.03			0.305±0.010
$\frac{\lambda_{pp}+\lambda_0}{\lambda_e}(10^{-4})$	0.91[h]			$1.12_{-0.46}{}^{+0.77}$	1.06±0.11			1.59 ±0.05
Yield at saturation	$n_\mu=0.025$ ±0.004	$n_\gamma=0.34$ ±0.06		$n_\mu=0.0264$ ±0.0035	$n_\gamma=0.33$ ±0.08			$n_\gamma=0.140$ ±0.024
Method	H_2 bubble chamber	H_2 target time to height converter	95% D_2 bubble chamber	H_2 bubble chamber	H_2 target time to height converter	High pressure diffusion chamber	H_2 target time to height converter	H_2 target digitron

[a] See Ref. 6.
[b] See Ref. 9.
[c] See Ref. 21.
[d] See Ref. 5.
[e] See Ref. 10.
[f] See Ref. 23.
[g] See Ref. 22.
[h] Assuming $c=40$ ppm.

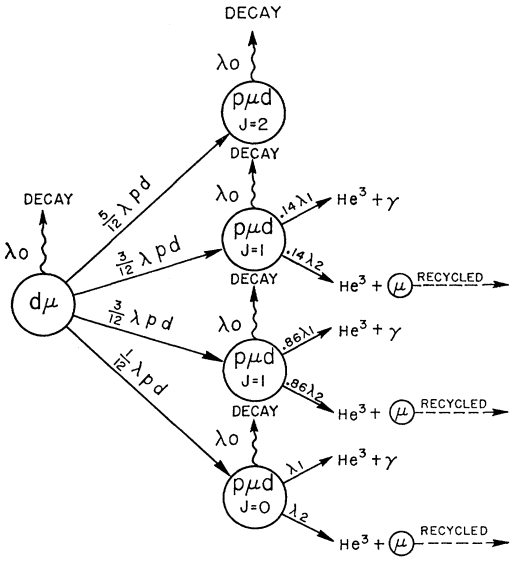

FIG. 2. Schematic diagram of the formation and decay of the four hyperfine states of the $p\mu d$ molecule. The formation rates of the hyperfine states, $\{(2J+1)/\Sigma_J(2J+1)\}\lambda_{pd}$ are based on the assumption that the states are populated statistically. J is the total spin of the muon, the proton, and the deuteron. The fusion rates are based on the assumption that fusion takes place only when the proton and deuteron are in a spin $\frac{1}{2}$ state.

where $\lambda_f=\lambda_1+\lambda_2$, the total fusion rate, and $\alpha=c\lambda_e+\lambda_{pp}$. For the saturated case when $c\lambda_e\gg\lambda_{pp}$, λ_{pd}, and λ_f, Eq. (4) becomes

$$(d/dt)n_\gamma(t)=[\lambda_1\lambda_{pd}/(\lambda_f-\lambda_{pd})]e^{-\lambda_0 t}\{e^{-\lambda_{pd}t}-e^{-\lambda_f t}\}, \quad (5)$$

a simple parent-daughter decay curve.

By measuring the yield of gamma rays as a function of time and fitting Eq. (4) or (5) to the results, values for the various rates can be determined. For the saturated case the determination of the two rates is straightforward, the rise of the yield curve determining a fast rate and the decay of the yield curve determining a slower rate. Since the equations are symmetric in λ_{pd} and λ_f, an additional experiment, discussed below, is necessary to determine that λ_{pd} is the fast rate and λ_f is the slow rate. For low deterium concentrations the yield curves still fall at a rate determined by λ_f but the rise is slower than for the saturated case. This reflects the fact that the muon spends some time in the μp atomic state whereas at saturation the lifetime of this state is very short. By analyzing the rate of rise of the curve at dilute deuterium concentrations λ_{pp} is extracted. It is useful to consider the expression for the mean elapsed time for the detection of a gamma ray from Eq. (4)

$$\langle t\rangle=\frac{1}{n_\gamma}\int_0^\infty t\frac{d}{dt}n_\gamma(t)dt$$
$$=\frac{1}{c\lambda_e+\lambda_{pp}+\lambda_0}+\frac{1}{\lambda_{pd}+\lambda_0}+\frac{1}{\lambda_f+\lambda_0}. \quad (6)$$

The terms are the lifetimes of the μp, μd, and $p\mu d$ systems, respectively.

While the above formulas are useful for demonstrating the main features of the analysis, it is emphasized that the actual analysis included the effects of muon recycling and hyperfine levels.

C. Hyperfine Structure of the $p\mu d$ Molecule

The fusion process is assumed to be a magnetic dipole transition in which a proton and a deuteron, in an orbital S state, with a total spin of $\frac{1}{2}$ go to the ground state of He^3 which is a spin $\frac{1}{2}S$ state. All other processes are much less likely.[7] The $p\mu d$ molecule has four spin states, $J=2$, 1, 1, and 0, each of which is some mixture of proton and deuteron total spin $\frac{1}{2}$ and $\frac{3}{2}$. The separation between the levels is much greater than the level widths so we must view the fusion process as proceeding from four independent states, each state having a different lifetime. The lifetimes are determined by the probability of fusion taking place for the given state. This in turn is determined by the probability that the proton and the deuteron are found in that state with a total spin $\frac{1}{2}$. For $J=2$, the proton and the deuteron always have total spin $\frac{3}{2}$; for $J=0$ their spin is always $\frac{1}{2}$; for the higher energy $J=1$ state their spin is $\frac{1}{2}$ 86% of the time; while for the lower energy $J=1$ level, their spin is $\frac{1}{2}$ 14% of the time.[1] Figure 2 summarizes these assignments. We have assumed that the various levels are populated statistically.[8] The intrinsic fusion rate for the spin $\frac{1}{2}$ state is taken to be λ_f, and the fusion rate for the $\frac{3}{2}$ state has been assumed to be zero. With these assumptions Eq. (2) must be replaced by

$$n_\gamma=\left(\frac{c\lambda_e}{c\lambda_e+\lambda_{pp}+\lambda_0}\right)\left(\frac{\lambda_{pd}}{\lambda_{pd}+\lambda_0}\right)\left(0.25\frac{0.14\lambda_1}{0.14\lambda_f+\lambda_0}+0.25\frac{0.86\lambda_1}{0.86\lambda_f+\lambda_0}+0.083\frac{\lambda_1}{\lambda_f+\lambda_0}\right). \quad (7)$$

Equation (7) predicts a yield of gamma rays per muon at deuterium saturation of about $(0.25+0.08)\lambda_1/(\lambda_f+\lambda_0)\simeq 11\%$. Earlier measurements[9,10] of a 34% yield are consistent with fusion taking place from all states of the molecule, since from Eq. (2) the yield at saturation is determined mainly by the factor $\lambda_1/(\lambda_f+\lambda_0)\simeq 33\%$. The predicted hyperfine effect on

[7] S. Cohen, D. L. Judd, and R. J. Riddell, Phys. Rev. **119**, 397 (1960).

[8] Calculations indicate that the $p\mu d$ molecule is formed in an $L=1$ rotational state, but not so quickly as to prevent the hyperfine mixing in the $L=1$ state ($\sim 10^{-13}$ sec^{-1}). It might appear that such spin-rotation mixing could disturb the statistical population of the final spin states. It can be shown in a general way, however, that provided the initial μd atom has statistical spin population, the population of the $p\mu d$ final states is statistical.

[9] A. Ashmore, B. Nordhagen, K. Strauch, and B. M. Townes, Proc. Phys. Soc. (London) **71**, 161 (1958).

[10] E. Bleser, L. Lederman, J. Rosen, J. Rothberg, and E. Zavattini, Phys. Rev. Letters **8**, 128 (1962).

the time distribution curves is small and our data are not sensitive to it. In order to test the assumptions of this section we remeasured the absolute yield of gamma rays and looked for an unusual effect predicted by Wolfenstein.[11]

If fusion takes place when the proton and the deuteron are in a total spin $\frac{1}{2}$ state, Wolfenstein has suggested[11] that there should be an enhanced yield of gamma rays from liquid hydrogen containing large deuterium concentrations. If there is sufficient deuterium present, the muons will transfer from spin $\frac{3}{2}$ to spin $\frac{1}{2}$ states by jumping from one deuteron to another in a process analogous to the depolarizing of muons in normal liquid hydrogen. A muon bound to a deuteron in a total spin $\frac{1}{2}$ state cannot transfer to a deuteron in a spin $\frac{3}{2}$ state since the thermal energy is much less than hyperfine splitting energy (0.046 eV). Gershtein[11] has calculated the transfer rate in liquid deuterium to be

$$W \approx 7\times 10^6 \text{ sec}^{-1}. \tag{8}$$

If the $p\mu d$ molecules are formed only from μd atoms of spin $\frac{1}{2}$, the population of the hyperfine states will no longer be statistical. The relative populations will be zero for the $J=2$ state, 0.39 and 0.36 for the two $J=1$ states and 0.25 for the $J=0$ state.[12] With these assumptions the yield of gamma rays is

$$n_\gamma = \frac{c\lambda_e}{c\lambda_e+\lambda_{pp}+\lambda_0}\frac{(1-c)\lambda_{pd}}{(1-c)\lambda_{pd}+\lambda_0}\left\{0.39\frac{0.14\lambda_1}{0.14\lambda_f+\lambda_0} + 0.36\frac{0.86\lambda_1}{0.86\lambda_f+\lambda_0} + 0.25\frac{\lambda_1}{\lambda_f+\lambda_0}\right\}. \tag{9}$$

Using Eqs. (8) and (9) we calculate that at $c=25\%$ the yield is enhanced by a factor

$$n_\gamma(25\%)/n_\gamma(0.72\%) = 1.18. \tag{10}$$

This experiment was undertaken with the aims of improving the knowledge of the various molecular rates, distinguishing between λ_f and λ_{pd}, reexamining the absolute yield and looking for an enhanced yield at higher deuterium concentrations.

III. EXPERIMENTAL APPARATUS

The experimental setup was identical with that described in the preceding paper[2] with regard to the high-purity liquid-hydrogen target, the shielding, the muon beam, and the electronics for counting the beam and the decay electrons. In order to count fusion gamma rays, one of the neutron counters was replaced by a sodium iodide crystal, 5 in. in diameter by 4 in. thick, viewed with an EMI 9530B 5-in. photomultiplier.

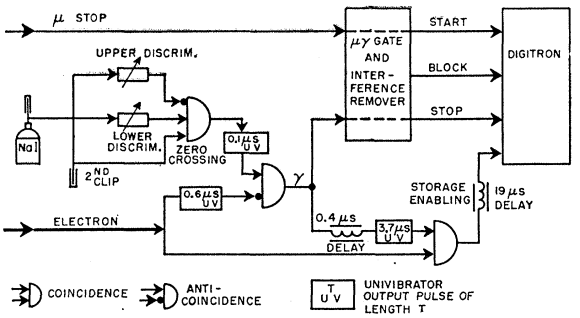

FIG. 3. Schematic diagram of the fusion gamma-ray counting electronics.

A. Electronics

The electronic logic is shown in Fig. 3. A single-channel pulse-height analyzer consisting of an upper and lower discriminator with their outputs in anticoincidence was used to limit the accepted pulses to an energy range of 3.9 to 6.4 MeV. The sodium iodide pulse was clipped twice and the zero crossing point used in order to measure the time of the pulse to within 10 nsec. A gamma ray was determined by a coincidence between the single-channel analyzer and the zero crossing circuit vetoed by the anticounters. This "gamma" pulse was sent to the digitron[13] which can be regarded as a clock to measure the time interval between a "mu stop" and a "gamma." The digitron output was stored in a pulse-height analyzer which yielded the number of "gammas" that occurred in successive 30-nsec intervals following the "mu stop" counts. The digitron and the "interference remover" circuitry which eliminated biases due to the simultaneous stopping of several muons are described in the succeeding paper[14] which reports a precise measurement of the muon lifetime using this equipment.

Included in the logic was the requirement that a "gamma" count be followed by a count in one of the four anticounters. This "delayed e" requirement was based on the assumption that for a real gamma ray from a fusion reaction, the muon still existed and would eventually decay into an electron. If "gamma" was from electron bremsstrahlung, there would be no electron following it within the "delayed e" gate which came 0.4 μsec after the "gamma" and was 3.7 μsec long. The "delayed e" requirement greatly reduced the background and permitted the observation of fusion γ rays

[11] L. Wolfenstein, *Proceedings of the 1960 Conference on High Energy Physics at Rochester* (Interscience Publishers, Inc., 1960), p. 533. S. S. Gershtein, Zh. Eksperim. i Teor. Fiz. **40**, 698 (1961) [English transl.: Soviet Phys.—JETP **13**, 488 (1961)].

[12] Gershtein's calculation ignores the possible effects due to the hyperfine mixing in the $L=1$ $p\mu d$ state (see Ref. 8). Note for example that Gershtein's solution has zero population for the $J=2$ state. It is possible, however, for the spin $\frac{1}{2}\mu d$ system to combine with a proton to form $p\mu d$ with spin 1, and by magnetic interaction in the $L=1$ state, precess into a spin 2 configuration. We thank L. Wolfenstein for pointing out this effect.

[13] W. LeCroy (to be published); R. A. Swanson, Rev. Sci. Instr. **31**, 149 (1960); R. A. Lundy, Phys. Rev. **125**, 1686 (1962).

[14] S. L. Meyer, E. W. Anderson, E. J. Bleser, L. M. Lederman, J. L. Rosen, J. E. Rothberg, and I. T. Wang, Phys. Rev. **132**, 2693 (1963).

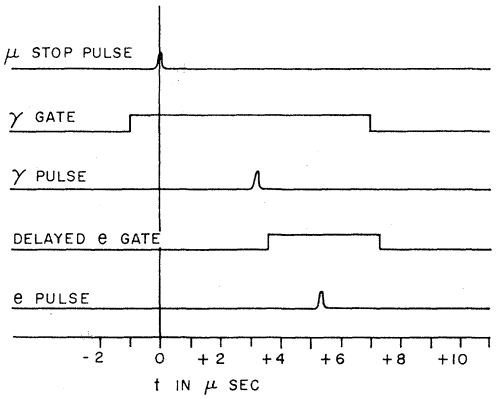

FIG. 4. Timing requirements for acceptance of a fusion gamma ray event. A pulse on the "μ stop" line opens an 8 μsec gate through which a pulse on the "γ" line must pass. The gamma pulse opens a "delayed e" gate through which a pulse on the electron line must pass. If these conditions are not met or if there are additional pulses on the μ or γ lines, the event is rejected.

for very low deuterium concentrations. Figure 4 is a diagram of the timing requirements of the electronics.

B. Sodium Iodide Detector

The energy window of the single-channel pulse-height analyzer was set between 3.9 and 6.4 MeV using the 4.43-MeV carbon gamma ray from a plutonium-beryllium source, and the 6.13-MeV gamma[15] from $O^{16}(n,p)N^{16} \xrightarrow{\beta} O^{16*}$. Figure 5 shows spectra from the two sources and from the fusion gamma ray observed during the experiment. The measured energy is 5.53 $\pm$0.05 MeV which compares with an expected value of 5.493$\pm$0.012 MeV.[16]

The efficiency of the sodium iodide crystal for detecting 6.14 MeV gamma rays was measured at the Columbia University Van de Graaff,[17] using the reaction $F^{19}(p,\alpha\gamma)O^{16}$ which has a resonance at 340 keV, giving 6.14-MeV gamma rays and an equal number of 1.8-MeV alpha particles.[18] The final result, corrected for the energy difference of the fusion and oxygen gamma rays, and for small geometrical effects, is that the 5-in. diameter by 4-in. thick sodium iodide crystal detected (1.65$\pm$0.20)% of the 5.5-MeV gamma rays. The crystal face was 6.7 in. from the center of the target and only gamma rays losing more than 3.9 MeV in the crystal were counted.

[16] We thank Dr. W. Frati for the loan of his activation apparatus. This consisted of a high-speed pumping system for circulating irradiated water from inside the synchrocyclotron shielding wall to the NaI detector position. See W. Frati and J. Rainwater, Phys. Rev. **128**, 2360 (1962).

[16] C. Li, W. Whaling, W. A. Fowler, and C. C. Lauritsen, Phys. Rev. **83**, 512 (1951).

[17] R. C. Cohen (to be published). We are grateful to Mr. Cohen for sharing his equipment with us and to the experimentors at the Van de Graaff Generator in Pegram Laboratory at Columbia University for helping us with the calibration.

[18] G. M. Griffiths, E. A. Larson, and L. P. Robertson, Can. J. Phys. **40**, 402 (1962).

C. Deuterium

The procedure for adding deuterium to the target was to bleed off 10 cu ft at STP of the pure hydrogen gas into a vacuum tank; admit a measured amount of deuterium to the palladium purifier; open the output of the purifier to the target; flush with 10 cu ft at STP of protium to carry the deuterium through the heat exchanging system into the target. The amount of deuterium admitted to the purifier was measured in a 120 cc volume at pressures up to 75 psi. This method gave an upper limit on the concentration of deuterium in the target since it was possible that some did not enter the target and was left dissolved in the palladium or condensed in the cooling coils.

IV. RESULTS

A. Data Analysis

The data consist of the absolute yield and the time distribution of fusion gamma rays for twelve different deuterium concentrations. A first set of runs was taken at deuterium concentrations of 1, 9, 22, 62, 131, 264, 515, and 7200 deuterons per one million protons. A second set of runs was taken starting with commercial cylinder hydrogen which was passed through the palladium purifier so that it was of high purity, but having a normal deuterium content of 40 ppm.[19] Additional runs were then made at 40, 282, 3200, and 250 000 ppm.

Table IV summarizes all the runs. The value of the

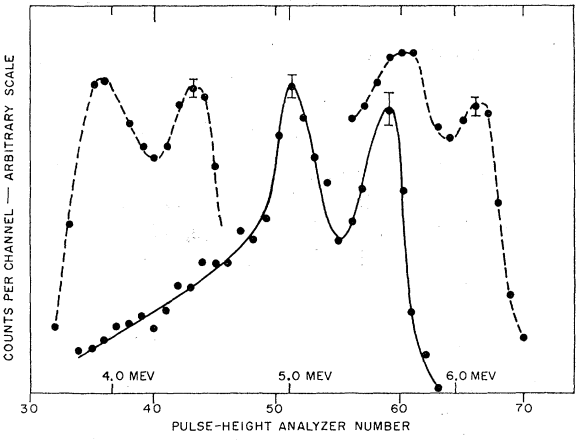

FIG. 5. Pulse height spectrum of the 5.5-MeV fusion gamma ray and, in dashed lines, of the 6.13-MeV oxygen gamma ray and the 4.43-MeV carbon gamma ray.

[19] Hydrogen in sea water has 150 ppm of deuterium but commercial cylinder hydrogen prepared by electrolysis normally has only 40 ppm. Thus the Chicago measurement of 40$\pm$15 ppm deuterium is to be expected and for the Berkeley data, normal conditions can be interpreted as 40 ppm rather than 150 ppm. The exact deuterium concentration of cylinder hydrogen depends on the manufacturer and the conditions at which he operates his electrolytic cells. A measurement of a sample from a cylinder of prepurified grade hydrogen of The Matheson Company gave a value of 43.5$\pm$2.0 ppm.

TABLE IV. Summary of experimental runs.

c (deuterium concentration) in ppm	"Mu stop" counts in 10^6	Fusion gamma rays	Ratio of column 3 to column 2
1	19.342	254	13.1
9	43.655	1394	32.0
22	86.635	6948	80.5
62	39.315	6672	169.7
131	18.473	4144	224.3
264	27.865	10 845	389.2
515	25.382	11 830	466.7
7200	34.503	20 094	582.3
40	18.700	2375	127.0
282	13.647	5334	390.8
3200	76.124	43 802	575.4
250 000	28.566	19 677	688.8

deuterium concentration is determined from the known volumes of the target and sampling volume and the pressure of deuterium gas to which the sampling volume was filled. Since these numbers are well known, the tabulated deuterium doses are very definite upper limits on the concentration of deuterium in the target. From the results shown below it is apparent that the concentration value of 131 ppm for the fifth run is in error and the actual value is about 100 ppm. We believe this discrepancy results from the fact that in this case the flushing of the deuterium through the purifier was insufficient.

Figure 6 shows the gamma yield plotted against the deuterium concentration. The experimental points are from the data in Table IV. The curve is calculated from Eq. (7) using the values determined below for the molecular rates. It is seen that the yield saturates when $c\lambda_e$ is greater than $\lambda_{pp}+\lambda_0$ and that the point at 25% deuterium has a greater yield than the 1% case (the Wolfenstein-Gershtein effect, Sec. IV-B). Figure 7 is an expansion of Fig. 6 in the region of lower concentrations.

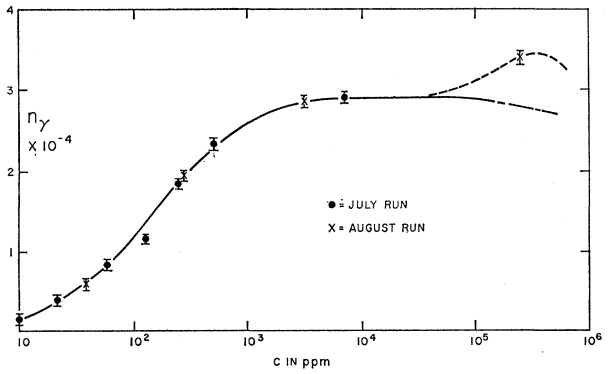

FIG. 6. Plot of n_γ, the total yield of gamma rays normalized to 50×10^6 "mu stop" counts, against the log of c, the deuterium concentration. The solid curve is computed from Eq. (7) using the parameters determined in this experiment. The curve — — — shows the decrease in yield when the factor $\lambda_{pd}/(\lambda_{pd}+\lambda_0)$ is replaced by $\lambda_{pd}(1-c)/\{\lambda_{pd}(1-c)+\lambda_0\}$ which is correct when c approaches 1. The curve – – – – – shows the expected behavior of the yield when the Wolfenstein-Gershtein effect is also included.

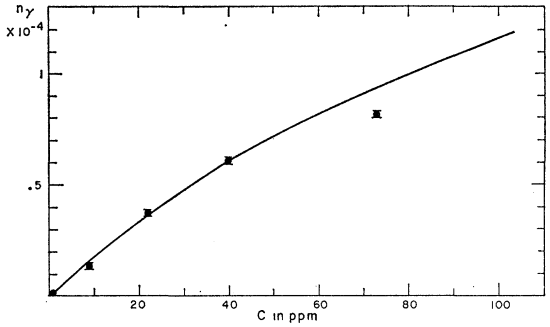

FIG. 7. Plot of n_γ, the total yield of gamma rays normalized to 50×10^6 "mu stop" counts against c, the deuterium concentration, for small values of c. This plot determines that the deuterium free case is actually at a deuterium concentration of about 1 ppm.

It shows the linear increase of the yield with deuterium concentration at very low concentrations. From this plot, we determine that the deuterium concentration of the initial point was less than 1 ppm. For this initial point the background subtraction is a large correction, but it is well understood and is based on the counts that come before zero time. If no background is subtracted from the initial concentration data the maximum deuterium concentration is still only 3 ppm.

If Eq. (7) is inverted we have

$$\frac{1}{n_\gamma}=\frac{1}{K}\left(1+\frac{\lambda_{pp}+\lambda_0}{\lambda_e}\frac{1}{c}\right). \tag{11}$$

Thus, $1/n_\gamma$, plotted versus $1/c$, gives a straight line shown in Fig. 8. The slope divided by the intercept of this line gives[20]:

$$(\lambda_{pp}+\lambda_0)/\lambda_e=(1.59\pm0.05)\times10^{-4},$$

[20] This result is different from that of Ref. 10 of $(1.06\pm0.11)\times10^{-4}$. Since for both cases the data fall along a straight line, the conclusion is that there is a systematic error in the concentration. The volumes and pressure gauges used in the present experiment were all checked and found to be correct. Therefore, we conclude that for this experiment the reported deuterium concentrations are very good upper limits. It is possible for this experiment that the process of adding deuterium to the chamber was inefficient—that a significant fraction of the deuterium was left dissolved in the palladium or condensed in the heat exchangers. An error of this sort would explain the difference in the results. However, the more likely explanation is that the major part of the difference can be attributed to the earlier experiment having a higher deuterium concentration. The deuterium adding process was such that deuterium gas might have been left in the manifold and carried into the target with the hydrogen gas used for flushing. A process of this sort would not have been apparent in the data from the few concentrations studied. The results of the present experiment seem preferable to those of the previous experiment since there are more data points taken over a wider range of concentrations; the results of two different sets of runs agree, and most importantly, the results for normal cylinder hydrogen, containing 40-ppm deuterium, agree with those for other concentrations. Mr. Irving Sucher in the laboratory of Dr. D. Rittenberg at the Columbia-Presbyterian Medical Center has very kindly analyzed hydrogen samples from all of our runs for their deuterium concentrations. His results are in general agreement with the expected values, but since the samples we provided were not equilibrium samples of H_2, D_2, and HD we cannot attach too much significance to the results.

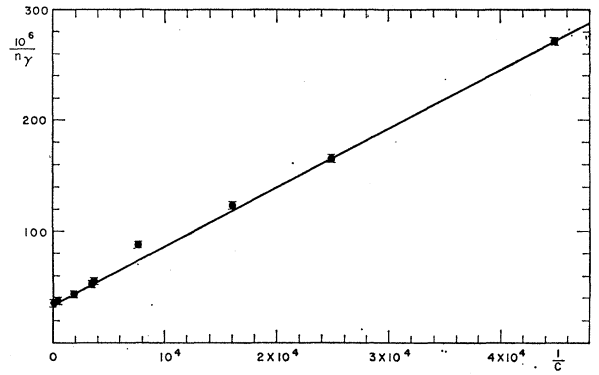

FIG. 8. Plot of $10^6/n_\gamma$ against $1/c$, where

$$\frac{10^6}{n_\gamma}=\frac{1}{K}\left(1+\frac{\lambda_{pp}+\lambda_0}{\lambda_e}\frac{1}{c}\right).$$

The straight line is a least-squares fit to the points, excluding the point at $c=131$ ppm. The fitted line is

$$10^6/n_\gamma=(5.28\pm0.02)\times10^{-3}(1/c)+33.7\pm0.5.$$

where a 2% correction, derived in Appendix I, to take account of recirculated muons, has been included.

Typical time distributions of the fusion gamma rays following the stopping of a muon in the target are shown in Figs. 9, 10, and 11.

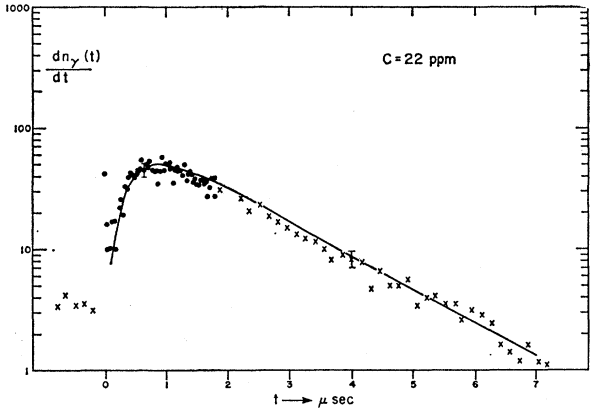

FIG. 9. Log plot of the time distribution of the fusion gamma rays, $(d/dt)n_\gamma(t)$, for a deuterium concentration, c, of 22 ppm. The data points are raw data from the digitron normalized to 50×10^6 "mu stop" counts. The dots are individual 30-nsec digitron channels. The crosses are averages over five channels. The curves have been determined by the method described in the text.

The data, as shown, have been normalized but are otherwise uncorrected. For the analysis a background subtraction is made. The background is attributed to a flat background of gamma rays, some of which accidentally came after a real muon stopped in the hydrogen but before its decay electron was detected. This background thus has a time dependence, a decay rate equal to the muon decay rate. Its magnitude can be estimated from the counts that come before zero time. These accidental counts before zero time are shown in the figures, averaged over five channels. Also apparent in the runs at the lower deuterium concentrations is a small "spike" at zero time. This is due to a muon stopping in a wall and giving a prompt mesic x ray. The "zero-time spike" clearly defines zero time and demonstrates the one channel resolution of the digitron.

Instead of Eq. (4) the equations fitted to the experimental data were the exact set (A5) to (A10), which include the recirculation of the conversion muon and

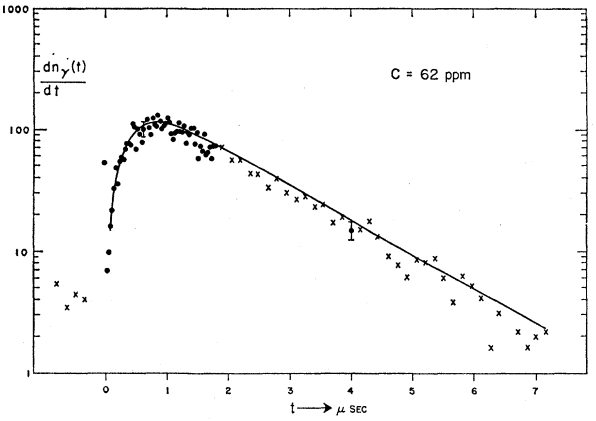

FIG. 10. Same as Fig. 9, except for a deuterium concentration, c, of 62 ppm.

the hyperfine structure of the $p\mu d$ molecule. They were integrated numerically on an IBM 7090 to give a time spectrum of fusion gamma rays which was compared with the experimental points to give a value for χ^2. The parameters were varied to minimize χ^2. The analysis procedure was to use the two runs for which the yield was saturated ($c=3200$ and 7200 ppm) to determine λ_f, λ_{pd} and the normalization. For these runs λ_{pp} and λ_e can be ignored as is seen from Eq. (5). The results are not sensitive to the exact value of λ_2/λ_1 which was set

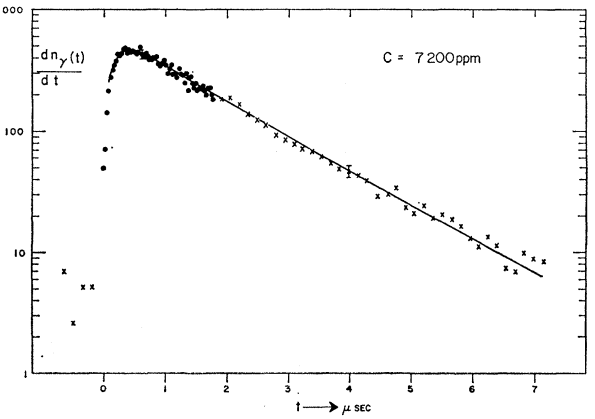

FIG. 11. Same as Fig. 9, except for a deuterium concentration, c, of 7200 ppm.

TABLE V. Values of λ_{pp} and λ_e.

C in ppm	λ_{pp} (10^6 sec^{-1})	λ_e (10^{10} sec^{-1})	χ^2	$\langle\chi^2\rangle$
9	1.89±0.20	1.21±0.10	52.3	45
22	1.98±0.08	1.56±0.06	157.3	127
62	1.98±0.09	1.48±0.06	161.2	134
131	1.93±0.13	1.14±0.06	78.3	111
(99)		1.51±0.08		
264	1.75±0.10	1.33±0.05	224.1	155
40	1.88±0.16	1.49±0.10	71.6	87
282	1.74±0.12	1.40±0.10	105.5	139
Mean values	1.89±0.20	1.43±0.13		

equal to 0.2. The fitted values are

$$\lambda_{pd}=(5.8\pm0.3)\times10^6\ \text{sec}^{-1},$$
$$\lambda_f=(0.305\pm0.010)\times10^6\ \text{sec}^{-1},$$
$$n_{\mu p}(t=0)=0.0054\times\text{"mu stops."}$$

The analysis of the dilute deuterium data determined the quantities λ_{pp} and λ_e in the following manner. The values of λ_{pd}, λ_f and the normalization were fixed at the values determined above. The value of $c\lambda_e/(c\lambda_e+\lambda_{pp}+\lambda_0)$ as determined from Eq. (7) and the experimental integrated yields was used as an additional constraint in the χ^2 curve fitting. Thus the χ^2 minimizing routine had only one degree of freedom. Table V gives values of λ_{pp} corresponding to the minimum χ^2 values for the different runs and a final weighted average. The value of λ_{pp} is determined without any dependence on our knowledge of c. Table V also lists values for λ_e derived from the value of $c\lambda_e$ found from the χ^2 fitting and the value of c measured from the deuterium filling procedure. The final value for λ_e is a weighted average which does not include the values for the runs at $c=131$ ppm which we believe to have an incorrect value for c and at $c=9$ ppm. Any uncertainty in the deuterium concentration affects only the value of λ_e. The good agreement of the results for λ_e suggests that the values of c determined from the filling procedure are correct. Typical computed curves using the measured rates are shown in Figs. 9, 10, and 11.

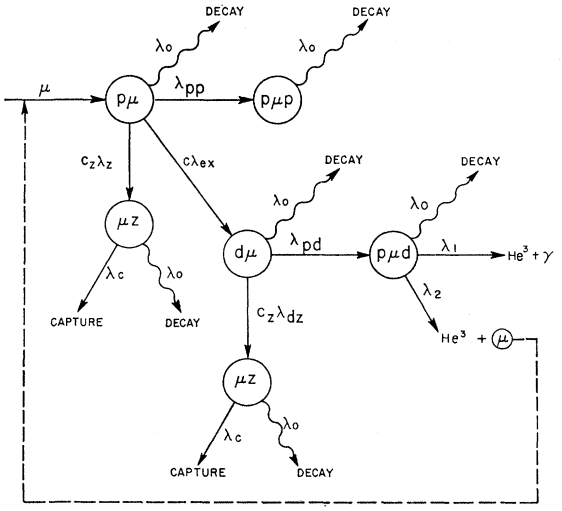

FIG. 12. Schematic diagram of the steps leading to a fusion event and of the important alternate steps, when the impurity concentration is not negligible.

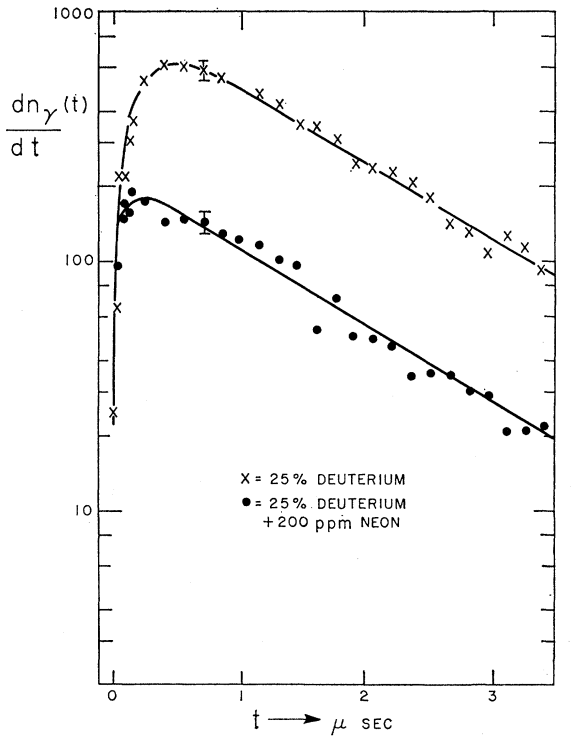

FIG. 13. Log plot of the time distribution of fusion gamma rays $(d/dt)n_\gamma(t)$ for the case of 25% deuterium concentration and for that case with 200-ppm neon added.

B. Wolfenstein-Gershtein Effect

Increasing c to 25% we measure a clear increase in yield and find

$$\frac{n_\gamma(25\%)}{n_\gamma(0.72\%)}=1.17\pm0.01. \quad (12)$$

This result is in good agreement with the predicted value of 1.18 and indicates that the analysis of the fusion process in Sec. II-C is correct.

C. Neon

If a high Z impurity is added to the hydrogen the possible transfer processes are shown in Fig. 12. For high deuterium concentrations a good approximation to the yield of gamma rays as a function of time is given by

$$\frac{d}{dt}n_\gamma(t)=\frac{\lambda_f\lambda_{pd}}{(\lambda_{pd}+c_z\lambda_{dz}-\lambda_f)}e^{-\lambda_0 t}\{e^{-\lambda_f t}-e^{-(\lambda_{pd}+c_z\lambda_{dz})t}\}. \quad (13)$$

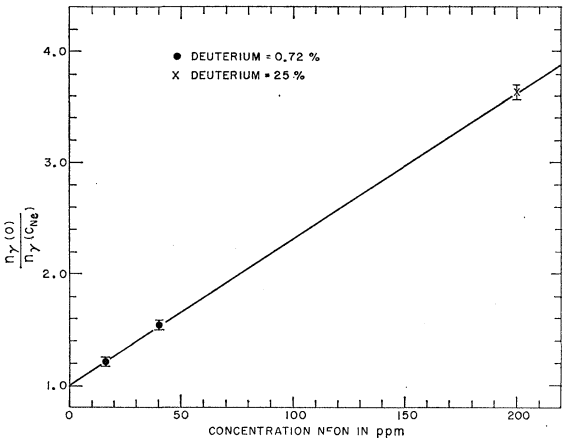

FIG. 14. Plot of $n_\gamma(0)/n_\gamma(C_{Ne})$ as a function of C_{Ne} where $[n_\gamma(0)/n_\gamma(C_{Ne})]=1+[\lambda_{Ne}/(\lambda_{pd}+\lambda_0)]C_{Ne}$. The slope of the line is $\lambda_{Ne}/(\lambda_{pd}+\lambda_0)=(1.3\pm0.2)\times10^4$.

An impurity will have two effects; decreasing the total yield and decreasing the observed lifetime associated with the μd atom.

Figure 13 shows a plot of the results from the 25% deuterium case and that case with 200 ppm of neon added. The yield has dropped, the slow rate has not changed and the fast rate has increased. Thus the fast rate observed is the disappearance rate of the μd atom and must be λ_{pd}. This result is in agreement with the Carnegie[21] and CERN[22] results but disagrees with Ref. 23.

For the deuterium saturated cases, we can assume that a muon transfers from a proton to a deuteron and then to the neon atom. The yield of gamma rays as a function of neon concentration c_{Ne} is:

$$n_\gamma = k\frac{\lambda_{pd}}{\lambda_{pd}+\lambda_0+c_{Ne}\lambda_{Ne}} \qquad (14)$$

and

$$\frac{1}{n_\gamma}=\frac{1}{k}\left\{\frac{\lambda_{pd}+\lambda_0}{\lambda_{pd}}+\frac{\lambda_{Ne}}{\lambda_{pd}}c_{Ne}\right\}.$$

Table VI gives the yields for neon added to the 0.72% and 25% deuterium cases. The inverse yields are plotted against neon concentration in Fig. 14. The slope of the straight line is $\lambda_{Ne}/(\lambda_{pd}+\lambda_0)=1.3\times10^4$. This gives the transfer rate of a muon from a deuteron to a neon atom as

$$\lambda_{Ne}=(8.1\pm1.0)\times10^{10}\ \text{sec}^{-1}.$$

This is in agreement with Schiff's result[5] of $(14\pm5)\times10^{10}$ sec^{-1}. Our result may be low due to the possibility that some of the neon may have condensed in the entrance tube of the target.

With a 1% concentration of neon in the hydrogen, the yield of fusion gamma rays goes to zero and we can conclude that all the muons are bound to neon. Measuring the time distribution of the decay electron gives a direct measurement of the disappearance rate of muons in neon. The measured disappearance rate is $(0.658\pm0.010)\times10^6$ sec^{-1}.

TABLE VI. Summary of experimental runs with neon in the hydrogen.

Deuterium concentration	C_{Ne} in ppm	"Mu stop" counts in 10^6	Fusion gamma rays	Ratio of column 3 to column 2
0.72%	0	34.503	20 014	580
	16	3.497	1659	475
	40	2.304	873	380
25%	0	28.566	19 677	689
	200	6.992	1195	171
	10 000	3.119	47	15

D. Absolute Yield

Table VII summarizes the measurement of the absolute yield. The final result is that the yield of fusion

TABLE VII. Absolute yield of gamma rays.

$Y_\gamma(c)=E\times G\times D\times B\times W\times F\times n$ ("mu stops")$\times n_\gamma$

$Y_\gamma(c)$ = number of fusion gamma rays counted at deuterium concentration c

E = absolute detection efficiency of sodium iodide crystal $=0.0165\pm0.0020$

G = fraction of fusion gamma rays accepted by digitron gate $=0.992\ \pm0.001$

D = fraction of decay electrons detected by delayed-e requirement $=0.45\ \pm0.05$

B = fraction of "mu stop" counts accepted by confusion elimination circuit $=0.914\ \pm0.010$

W = fraction of 5.5-MeV gamma rays not stopped by target walls $=0.926\ \pm0.004$

F = fraction of "mu stop" counts which are mesons stopping in the liquid hydrogen $=0.664\ \pm0.020$

n("mu stops") = total number of "mu stop" counts at concentration c

n_γ = fraction of muons that catalyze a fusion event giving a 5.5-MeV gamma ray

$Y_\gamma(c)=(0.00414\pm0.00069)\times n$("mu stops") $\times n_\gamma$

for

$$c=0.72\%$$
$$Y_\gamma(0.72\%)=20\,014\pm141$$
$$n(\text{"mu stops"})=(34.503\pm0.006)\times10^6$$

to give

$$n_\gamma=(14.0\pm2.4)\%$$

while the expected value is

$$n_\gamma=(11.4\pm0.5)\%$$

[21] J. G. Fetkovich, T. H. Fields, G. B. Yodh, and M. Derrick, Phys. Rev. Letters 4, 570 (1960).

[22] G. Conforto, S. Focardi, C. Rubbia, and E. Zavattini, Phys. Rev. Letters 9, 432 (1962) and Erratum in Phys. Rev. Letters 9, 525 (1962).

[23] V. P. Dzhelepov, M. Friml, S. S. Gershtein, YU. V. Kathyshev, V. I. Moskalev, and P. F. Yermolov, *Proceedings of the 1962 International Conference on High Energy Physics at CERN* (CERN Scientific Information Service, Geneva, 1962), p. 484.

gamma rays per muon stopped in liquid hydrogen is $(14.0\pm2.4)\%$ at 1% deuterium concentration. This is in fair agreement with the value of $(11.4\pm0.5)\%$ computed from Eq. (7) using the rates determined above. The present result disagrees with both our 1961 experiment[10] and the Liverpool[9] measurement (see Table III). With regard to the 1958 Liverpool measurements we can only point out that our experiment has benefitted from many technological improvements, viz. tenfold improvement in duty cycle, specially constructed H_2 target, purified muon beam, greatly reduced background, digital time sorter, and greater statistical accuracy. We believe we can account for the bulk of the discrepancy with our 1961 experiment more specifically. In that measurement the absolute yield was determined by comparison with the yield of $(2p\rightarrow 1s)$ 5.3-MeV mesonic x rays from Ta. The calibration was carried out with nonideal geometry and further, it was assumed that the yield of 5.3-MeV γ's was one per stopping muon. We find from our present calibration procedure and a much improved Ta measurement that the muonic 5.3-MeV x-ray yield is only $(58\pm10)\%$. This is, in itself, an interesting result. The bulk of the effect we attribute to the presence of nonradiative transitions, which we discuss in Appendix II.

V. DISCUSSION

A. Fusion Rate

We have measured the total fusion rate

$$\lambda_f=(0.305\pm0.010)\times10^6\ \text{sec}^{-1},$$

where $\lambda_f=\lambda_1+\lambda_2$, and λ_1 is the rate for a magnetic dipole transition yielding a gamma ray and λ_2 is the rate for an electric monopole transition which ejects the conversion muon.

Theoretical calculations[7] indicate that the magnetic dipole transition is the only significant process yielding gamma rays. It is assumed to take place from a state in which the proton and the deuteron have a total spin of $\frac{1}{2}$ and zero orbital angular momentum. Calculations also indicate that the internal conversion process takes place from the same state. If gamma and muon emission do proceed from the same states, the ratio of internal conversion muons to gamma rays equals λ_2/λ_1. Thus[5]

$$\frac{\lambda_2}{\lambda_1}=\frac{n_\mu}{n_\gamma}=\frac{0.0264\pm0.0035}{0.140\pm0.024}$$
$$=0.19\pm0.04. \qquad (15)$$

This gives

$$\lambda_1=(0.256\pm0.012)\times10^6\ \text{sec}^{-1},$$
$$\lambda_2=(0.049\pm0.010)\times10^6\ \text{sec}^{-1}.$$

Our result can be compared in principle with the recently measured low-energy s-wave cross section for the $D(p,\gamma)He^3$ reaction.[24] Most attempts at calculating λ_f have been based on using this cross section instead of evaluating the He^3 nuclear wave function [since this cross section was not then known, the cross section for the reaction $D(n,\gamma)H^3$ of the mirror nuclei was actually used]. Following Ref. 1, the low-energy cross section is given by

$$\sigma=R|\Psi(0)|^2/v,$$

where R is the reaction constant, $\Psi(0)$ is the wave function of the relative motion of the nuclei evaluated when the nuclei are separated by a distance less than the range of nuclear forces, and v is the relative velocity of the nuclei at infinity. The fusion rate is given by

$$\lambda_1=R|G(0)|^2,$$

where $G(0)$ is the wavefunction describing the relative motion of the nuclei in the $p\mu d$ molecule evaluated at zero separation of the nuclei.

From Ref. 24 the cross section for s-wave capture at 25 keV is

$$\sigma\{D(p,\gamma)He^3\}=(1.3\pm0.3)\times10^{-32}\ \text{cm}^2.$$

Using a simple Coulomb wavefunction for $\Psi(0)$ gives

$$|\Psi(0)|^2=2\pi\eta/(e^{2\pi\eta}-1).$$

At 25 keV $\eta=e^2/(\hbar v)=1.0$ and $|\Psi(0)|^2=1.16\times10^{-2}$. Thus $R=(2.5\pm0.6)\times10^{-22}$ cm^3/sec. Assuming the process is magnetic dipole and goes only from the total spin $\frac{1}{2}$ state this result must be increased by a factor of 3 for comparison with λ_1. Thus $|G(0)|^2=3.25\times10^{26}$ cm^{-3}. Only crude estimates[1] of $|G(0)|^2$ are to date available. These are made by barrier penetration calculations or by integrating the Schrodinger equation of the $p\mu d$ molecule for small pd separation to give values from 14 to 100×10^{26} cm^{-3}.

TABLE VIII. Results of this experiment.

$p\mu+d\xrightarrow{\lambda_e} d\mu+p$	$(1.43\pm0.13)\times10^{10}$ sec^{-1}
$p\mu+p\xrightarrow{\lambda_{pp}} p\mu p$	$(1.89\pm0.20)\times10^6$ sec^{-1}
$d\mu+p\xrightarrow{\lambda_{pd}} p\mu d$	$(5.8\pm0.3)\times10^6$ sec^{-1}
$p\mu d\xrightarrow{\lambda_f} He^3$	$(0.305\pm0.010)\times10^6$ sec^{-1}
$\dfrac{\lambda_{pp}+\lambda_0}{\lambda_e}$	$(1.59\pm0.05)\times10^{-4}$
n_γ at 1% deuterium	0.140 ± 0.024
$\dfrac{n_\gamma \text{ at } 25\%\ D_2}{n_\gamma \text{ at } 1\%\ D_2}$	1.17 ± 0.01
μ^- disappearance rate in neon	$(0.658\pm0.010)\times10^6$ sec^{-1}
$\mu d+\text{Ne}\xrightarrow{\lambda_{d\text{Ne}}}\mu\text{Ne}+d$	$(8.1\pm1.0)\times10^{10}$ sec^{-1}

[24] G. M. Griffiths, M. Lal, and C. D. Scarfe, Can. J. Phys. **41**, 724 (1963). We thank the authors for sending us a preprint.

B. Molecular Rates

The results of this experiment are summarized in Table VIII. Comparison with theory may be made by reference to Tables I and II. The molecular formation process has been viewed as an electric dipole transition with the ejection of a conversion electron from an initial S state to a bound state with rotational angular momentum equal to one. For the $p\mu p$ and $p\mu d$ molecules, the only bound states are the rotational $L=1$ state and the ground S state. The $p\mu d$ molecule makes a rapid transition to the ground state by electric dipole ejection of a conversion electron. The $p\mu p$ molecule remains in the metastable excited state.[1,7] The results of the muon capture experiment[2] are in accord with the $p\mu p$ molecule being in the metastable excited state. The calculated rates[1] for $p\mu p$ formation, $(3.7 \text{ or } 2.5)\times10^6$ sec^{-1}, are reasonably close to the measured value, 1.9×10^6 sec^{-1}, but agree better with the results of Ref. 22.

The calculated rates for $p\mu d$ formation take account only of the same dipole formation process. It is argued that the result for λ_{pd} must be lower than the result for λ_{pp} since the principal contribution to the matrix element comes from the classically forbidden region where the wave functions fall off with an exponential dependence on the reduced mass of the nuclei.[1] However, the measured value for λ_{pd} is three times greater than the result for λ_{pp}. An additional contribution to the $p\mu d$ molecular formation rate may come from the dipole moment associated with an asymmetry in the distribution of the nuclear charges with respect to the center of mass.

ACKNOWLEDGMENTS

We wish to thank the staff of the Nevis Laboratories for their generous support and to acknowledge the special contributions of Mr. W. LeCroy and Mr. W. Sippach who designed the digitron electronics.

APPENDIX I

Differential Equations

The differential equations giving the population, $n_a(t)$, of a state a at a time t derived from Fig. 1 are:

$$(d/dt)n_{\mu p}(t)=-(c\lambda_e+\lambda_{pp}+\lambda_0)n_{\mu p}(t)+\lambda_2 n_{p\mu d}(t); \quad \text{(A1)}$$

$$(d/dt)n_{\mu d}(t)=-(\lambda_{pd}+\lambda_0)n_{\mu d}(t)+c\lambda_e n_{\mu p}(t); \quad \text{(A2)}$$

$$(d/dt)n_{p\mu d}(t)=-(\lambda_1+\lambda_2+\lambda_0)n_{p\mu d}(t)+\lambda_{pd}n_{\mu d}(t); \quad \text{(A3)}$$

$$(d/dt)n_\gamma(t)=\lambda_1 n_{p\mu d}(t). \quad \text{(A4)}$$

If the recirculation of the muon following fusion is ignored, these equations are easily solved to give Eq. (4).

When the hyperfine states are included in the analysis, the differential equations derived from Figs. 1 and 2 are:

$$(d/dt)n_{\mu p}(t)=-(c\lambda_e+\lambda_{pp}+\lambda_0)n_{\mu p}(t)+0.14\lambda_2 n_{p\mu d1}(t)+0.86\lambda_2 n_{p\mu d1'}(t)+\lambda_2 n_{p\mu d0}(t); \quad \text{(A5)}$$

$$(d/dt)n_{\mu d}(t)=-(\lambda_{pd}+\lambda_0)n_{\mu d}(t)+c\lambda_e n_{\mu p}(t); \quad \text{(A6)}$$

$$(d/dt)n_{p\mu d1}(t)=-\{0.14(\lambda_1+\lambda_2)+\lambda_0\}n_{p\mu d1}(t)+\tfrac{1}{4}\lambda_{pd}n_{\mu d}(t); \quad \text{(A7)}$$

$$(d/dt)n_{p\mu d1'}(t)=-\{0.86(\lambda_1+\lambda_2)+\lambda_0\}n_{p\mu d1'}(t)+\tfrac{1}{4}\lambda_{pd}n_{\mu d}(t); \quad \text{(A8)}$$

$$(d/dt)n_{p\mu d0}(t)=-\{\lambda_1+\lambda_2+\lambda_0\}n_{p\mu d0}(t)+(1/12)\lambda_{pd}n_{\mu d}(t); \quad \text{(A9)}$$

$$(d/dt)n_\gamma(t)=0.14\lambda_1 n_{p\mu d1}(t)+0.86\lambda_1 n_{p\mu d1'}(t)+\lambda_1 n_{p\mu d0}(t). \quad \text{(A10)}$$

For the curve fitting analysis the time distribution of gamma rays was found by numerical integration of these equations on an IBM 7090.

Although these equations have not been solved to give an analytic expression for $(d/dt)n_\gamma(t)$, it is possible to derive an exact expression for the total yield n_γ' where

$$n_\gamma'=\int_0^\infty \frac{d}{dt}n_\gamma(t)dt. \quad \text{(A11)}$$

Let a be the probability that an initial muon results in a fusion gamma ray when recirculation is neglected. Let b be the probability that an initial muon results in a rejuvenated muon when recirculation is neglected. Then $a=n_\gamma$ from Eq. (7) and $b=\eta a$, where $\eta=\lambda_2/\lambda_1$. If n_0 is the number of muons that stop in the target, the effective number of muons, n_e, that might result in a fusion process is

$$n_e=n_0+bn_e=n_0/(1-b). \quad \text{(A12)}$$

The total yield of gamma rays is

$$n_\gamma'=an_e=an_0/(1-\eta a). \quad \text{(A13)}$$

From this equation the corrections necessary to Eq. (11) can be derived

$$\frac{1}{n_\gamma'}=\frac{1}{an_0}-\frac{\eta}{n_0}=\frac{1}{Kn_0}\left\{1+\frac{\lambda_{pp}+\lambda_0}{\lambda_e}\frac{1}{c}\right\}-\frac{\eta}{n_0}. \quad \text{(A14)}$$

Plotting $1/n_\gamma'$ as a function of $1/c$ gives for the ratio of the slope to intercept

$$\frac{S}{I}=\frac{\lambda_{pp}+\lambda_0}{\lambda_e}\{1-\eta K\}^{-1}, \quad \text{(A15)}$$

where K, defined by Eqs. (7) and (11), is 0.11 and η is 0.19 from Eq. (15).

APPENDIX II

Non-Radiative Transitions in Tantalum

The nonradiative (N.R.) muonic atom transition wherein the muon energy is imparted to an Auger electron is well known. This is a highly competitive process for transitions in levels of high principal

quantum number, but is not the effect observed here by many orders of magnitude. Nonradiative transitions in which muon energy is transformed into nuclear excitation have been observed for U and Th by Muhkin *et al.*[25] Dipole photoexcitation was postulated to explain this experiment, i.e.,

$$\mu(2p \text{ state})+\text{nucleus (ground state)} \xrightarrow[Q=6 \text{ MeV}]{E_1} \mu(1s \text{ state})+\text{nucleus (excited)}.$$

Zaretskii and Novikov[26] have theoretically analyzed this situation and obtained a formula relating the N.R. transition probability to the dipole photoexcitation cross section for 6-MeV photons. Insofar as a "reasonable" cross section can be inferred from existing photoexcitation data, the mechanism is plausible.

In the case of Ta, however, it is difficult to see how this process can be realized. The $2p \rightarrow 1s$ energy is 5.4 MeV while the neutron binding energy is 7.6 MeV. The Coulomb effect of the muon on the nucleus is not expected to reduce this binding energy appreciably. Since it is then impossible to excite the nucleus to a continuum state, the N.R. dipole process is ruled out.

We believe the most likely process to be

$$\mu(3d \text{ state})+\text{nucleus (ground state)} \xrightarrow[Q=9 \text{ MeV}]{E_2} \mu(1s \text{ state})+\text{nucleus (excited)}.$$

If the E_2 N.R. transition is competitive with the $3d \rightarrow 2p$ radiative transition, an absence of $2p \rightarrow 1s$ x-rays would result. Russell[27] has recently proposed and calculated this process. Again, the mechanism is plausible to the extent that a "reasonable" quadrupole photoexcitation cross section is used.

[25] A. I. Muhkin, M. J. Bulutz, L. N. Kondratiev, L. G. Landsburg, P. I. Lebedev, Yu. V. Obukliov, and B. Pontecorvo, *Proceedings of the 1960 Annual International Conference on High Energy Physics at Rochester* (Interscience Publishers, Inc., New York, New York, 1960), p. 550.

[26] D. F. Zaretskii and V. M. Novikov, Nuclear Phys. **28**, 177 (1961).

[27] J. E. Russell, Phys. Rev. **127**, 245 (1962).

PHYSICAL REVIEW VOLUME 132, NUMBER 6 15 DECEMBER 1963

Muon Capture in Neon*

J. L. Rosen, E. W. Anderson, E. J. Bleser,† L. M. Lederman,
S. L. Meyer, J. E. Rothberg,‡ and I-T. Wang
Columbia University, New York, New York

(Received 31 July 1963)

By exploiting the transfer process $(\mu^- p)+\text{Ne} \rightarrow p+(\mu^-\text{Ne})$, we have measured the disappearance rate of negative muons bound to neon nuclei. We find $\lambda=(0.658\pm0.010)\times10^6$ sec^{-1}.

A MEASUREMENT of the total rate of nuclear muon capture by neon has been carried out. The measurement was facilitated by the fact that muons stopped in liquid hydrogen with a relatively small admixture of neon, will form neon muonic atoms by irreversible transfer from hydrogen muonic atoms.[1]

Starting with pure hydrogen having a 25% D_2 concentration, we observed a yield of 0.16 fusion γ rays per stopped muon.[2] Upon the addition of 1% neon, the fusion γ-ray yield dropped to $(2\pm2)\times10^{-4}$, indicating that essentially all of the muons transferred to neon. The fusion γ yield as a function of time and neon and deuterium concentration was measured with a 33-Mc/sec digital time sorter (digitron). Simultaneously, the time spectrum of decay electrons from the (μNe) atoms was recorded with a 10-Mc/sec digitron. The electron data is shown in Fig. 1. The disappearance rate of muons is given by the slope of the exponential curve. A χ^2 analysis yields a value $\lambda_{\text{decay}}+\lambda_c=(0.658\pm0.010)\times10^6$ sec^{-1}. If we take the bound decay rate equal to 0.454×10^6 sec^{-1},

$$\lambda_c=(0.204\pm0.010)\times10^6 \text{ sec}^{-1}.$$

This is in fair agreement with the recently reported value of $(0.167\pm0.03)\times10^6$ sec^{-1} of Conforto, Rubbia, and Zavattini.[3] They used a similar technique for forming (μNe) but measured only the decrease in the time integrated yield of decay electrons.

In order to compare the result with other nuclei we interpolate the Primakoff curve as given in the compila-

* Work supported in part by the Office of Naval Research.

† Present address: Brookhaven National Laboratory, Upton, New York.

‡ Present address: Yale University, New Haven, Connecticut.

[1] M. Schiff and R. Hildebrand were the first to study this irreversible transfer process. M. Schiff, Nuovo Cimento **22**, 66 (1961).

[2] E. Bleser, E. W. Anderson, L. M. Lederman, S. L. Meyer, J. L. Rosen, J. E. Rothberg, and I-T. Wang, Phys. Rev. **132**, 2679 (1963).

[3] G. Conforto, C. Rubbia, and E. Zavattini, Phys. Rev. Letters **4**, 239 (1963).